

J/ψ production in proton-lead collisions at 8 TeV with the LHCb detector

Oleksandr Okhrimenko^{1,*} on behalf of LHCb Collaboration

¹ *Institute for Nuclear Research NAS of Ukraine, Kiev, Ukraine*

Abstract. The production of J/ψ mesons is studied in proton-lead collisions at a centre-of-mass energy per nucleon pair $\sqrt{s_{NN}} = 8.16$ TeV with the LHCb detector. The double differential cross-sections of prompt and nonprompt J/ψ production are measured as functions of the J/ψ transverse momentum and rapidity. Nuclear modification factors are determined. The results are compared with different theoretical calculations.

1 Introduction

The study of proton-nucleus collisions is important to disentangle the effects of quark-gluon plasma from non-deconfinement ones. The measurements of the production of prompt J/ψ and nonprompt J/ψ mesons are important ingredients for the understanding of the imprints of deconfinement in nucleus-nucleus collisions. They are based on 10 and 40 times larger integrated luminosities than the initial measurements with the 2013 p Pb and Pb p data samples, respectively, by the LHCb experiment at $\sqrt{s_{NN}} = 5$ TeV [1]. Furthermore, these results can be used to evaluate models, such as collinear factorisation with different nuclear parton distribution functions (nPDFs) [2], coherent energy loss [3] and the colour glass condensate model (CGC) [4], describing nuclear modifications in proton-nucleus collisions. In addition, the measurements are a natural reference for the measurement of $\phi(2S)$ and χ_c states, which will further clarify the modification of quarkonium production in proton-lead collisions at the TeV scale. In detail this analysis is described in Ref. [5].

2 Analysis Description and Results

The LHCb detector [6, 7] is a single-arm forward spectrometer covering the pseudorapidity range $2 < \eta < 5$, designed for the study of particles containing b or c quarks.

This analysis is based on data acquired during the 2016 LHC heavy-ion run, where protons and ^{208}Pb ions were colliding at a centre-of-mass energy per nucleon pair of $\sqrt{s_{NN}} = 8.16$ TeV. Since the energy per nucleon in the proton beam is larger than in the lead beam, the nucleon-nucleon centre-of-mass system has a rapidity in the laboratory frame of 0.465 (-0.465), when the proton (lead) beam travels from the vertex detector towards the muon chambers, which is denoted as p Pb (Pb p). Consequently, the LHCb detector covers two different acceptance regions: $1.5 < y^* < 4.0$ for p Pb and $-5.0 < y^* < -2.5$ for Pb p , where y^* is the rapidity in the centre-of-mass frame of the colliding

*e-mail: okhrimenko@kinr.kiev.ua

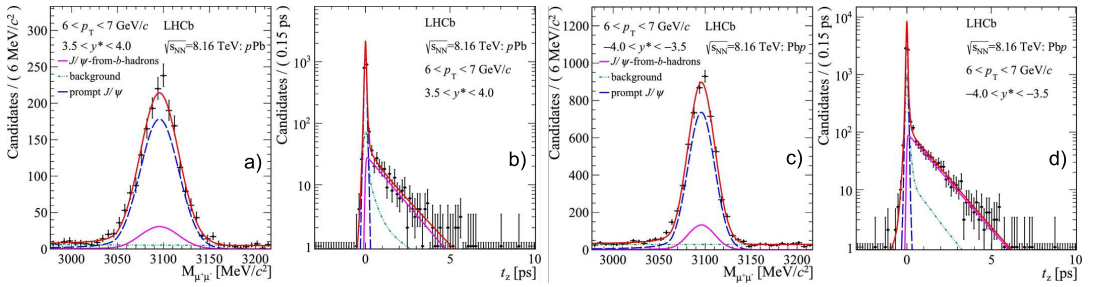


Figure 1. (a, c) Invariant mass and (b, d) pseudo proper time distributions for J/ψ candidates in the bin $6 < p_T < 7$ GeV/c and $3.5 < |y^*| < 4.0$ for the (a, b) p Pb and (c, d) Pb p samples respectively. The black circles with error bars represent the LHCb data. The red solid line is the total fit function, the blue dashed line is the prompt J/ψ signal component, the purple solid line is the nonprompt one and the green dashed line is the combinatorial background component.

nucleons, with the proton beam direction defined to be positive y^* . The data samples correspond to an integrated luminosity of 13.6 ± 0.3 nb $^{-1}$ of p Pb collisions and 20.8 ± 0.5 nb $^{-1}$ of Pb p collisions.

Candidate J/ψ are reconstructed through the $J/\psi \rightarrow \mu^+\mu^-$ decay channel. Each identified muon track is required to have $p_T > 750$ MeV/c, $2 < \eta < 5$ and to have a good-quality track fit. The two muon tracks of the J/ψ candidate must form a good-quality vertex, representing a tighter selection compared to the software trigger requirement. Also, only J/ψ candidates with an invariant mass $M_{\mu^+\mu^-}$ within 120 MeV/c 2 of the known value of the J/ψ mass (3097 MeV/c 2) are selected. The number of J/ψ candidates is extracted by fitting the invariant mass distribution, where the signal is described by a Crystal Ball function, and the combinatorial background by an exponential function (Fig. 1, a, c plots). Prompt J/ψ can be distinguished from nonprompt J/ψ by exploiting the pseudo proper time distribution (Fig. 1, b, d plots) defined as $t_z \equiv (z_{J/\psi} - z_{PV}) \cdot M_{J/\psi}/p_z$, where $z_{J/\psi}$ and z_{PV} are the coordinates along the beam axis of the J/ψ decay vertex position and of the primary vertex position, p_z is the z component of the J/ψ momentum and $M_{J/\psi}$ the known J/ψ mass. The t_z distribution of prompt J/ψ is described by a Dirac $\delta(t_z)$, and that of nonprompt J/ψ by an exponential function for $t_z > 0$. The background t_z distribution is described by an empirical function derived from the shape observed in the J/ψ upper mass sideband, $3200 < M_{\mu^+\mu^-} < 3250$ MeV/c 2 .

The double differential J/ψ production cross-section in each (p_T, y^*) bin is computed as

$$\frac{d^2\sigma}{dp_T dy^*} = \frac{N(J/\psi \rightarrow \mu^+\mu^-)}{\mathcal{L} \cdot \epsilon_{tot} \cdot \mathcal{B}(J/\psi \rightarrow \mu^+\mu^-) \cdot \Delta p_T \cdot \Delta y^*}, \quad (1)$$

where $N(J/\psi \rightarrow \mu^+\mu^-)$ is the number of reconstructed prompt or nonprompt J/ψ signal mesons, ϵ_{tot} is the total detection efficiency in the given kinematic bin, $\mathcal{B}(J/\psi \rightarrow \mu^+\mu^-) = (5.961 \pm 0.033)\%$ is the branching fraction of the decay $J/\psi \rightarrow \mu^+\mu^-$, $\Delta p_T = 1$ GeV/c and $\Delta y^* = 0.5$ are the bin widths and \mathcal{L} is the integrated luminosity. The total detection efficiency, ϵ_{tot} , is the product of the geometrical acceptance, and the efficiencies for charged track reconstruction, particle identification, candidate and trigger selections. Samples of simulated events are used to evaluate these efficiencies except for the track reconstruction and particle identification, which are determined in a data-driven approach. In the simulation, p Pb and Pb p minimum-bias collisions are generated using the Epos LHC [8] and J/ψ candidates from PYTHIA8 are injected into each event [9]. The measured double-differential cross-sections of prompt and nonprompt J/ψ in the p Pb and Pb p data samples are shown in Fig. 2, as a function of p_T for the considered y^* bins.

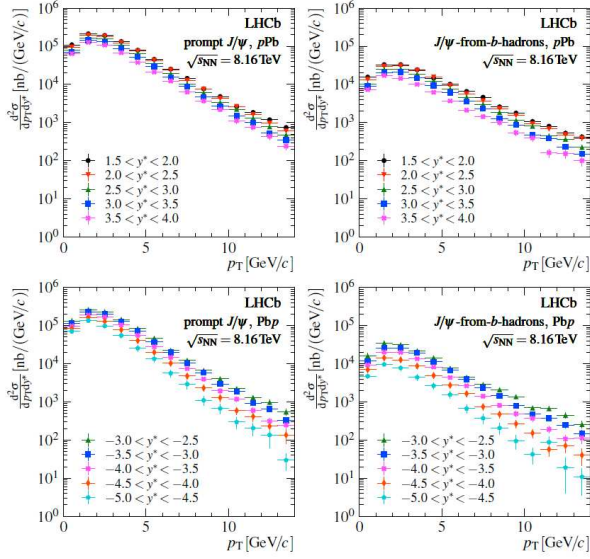


Figure 2. Production cross-section for (left column) prompt J/ψ and (right column) nonprompt J/ψ in (top row) $p\text{Pb}$ and (bottom row) $\text{Pb}p$ collisions as function of p_T for the considered y^* bins.

The nuclear modification factor $R_{p\text{Pb}}$ is computed from the prompt and nonprompt J/ψ production cross-sections in pp [10, 11] and $p\text{Pb}$ or $\text{Pb}p$ collisions using the following definition:

$$R_{p\text{Pb}}(p_T, y^*) \equiv \frac{1}{A} \frac{d^2 \sigma_{p\text{Pb}}(p_T, y^*) / dp_T dy^*}{d^2 \sigma_{pp}(p_T, y^*) / dp_T dy^*}, \quad (2)$$

where $A = 208$ is the mass number of the Pb ion, $d^2 \sigma_{p\text{Pb}}(p_T, y^*) / dp_T dy^*$ the J/ψ production cross-section in $p\text{Pb}$ or $\text{Pb}p$ collisions and $d^2 \sigma_{pp}(p_T, y^*) / dp_T dy^*$ the J/ψ reference production cross-section in pp collisions at the same nucleon-nucleon centre-of-mass energy.

The results obtained are shown in Fig. 3 (top and bottom rows denotes to prompt and non-prompt J/ψ , respectively). A suppression of prompt J/ψ production compared to pp collisions of up to 50% (25%) in $p\text{Pb}$ ($\text{Pb}p$) at the lowest p_T is observed. In both configurations, the nuclear modification factor approaches unity asymptotically at the highest p_T . Theoretical calculations for the nuclear modification factor based on nPDFs, coherent energy loss as well as the CGC model can account for the majority of the observed dependences. For the first time, beauty-hadron production is measured through inclusive decays $b \rightarrow J/\psi X$ precisely down to $p_T = 0$ at the LHC in $p\text{Pb}$ and $\text{Pb}p$ collisions. In $p\text{Pb}$, a weak suppression at the lowest p_T is observed, whereas in $\text{Pb}p$ no significant deviation from unity in the nuclear modification factor is found. This weak modification of beauty production in proton-ion collisions is an important ingredient for the investigation of the modifications of beauty production in heavy-ion collisions.

3 Conclusions

The differential production cross-sections of prompt and nonprompt J/ψ in $p\text{Pb}$ and $\text{Pb}p$ collisions at $\sqrt{s_{NN}} = 8.16$ TeV are measured in the range $0 < p_T < 14$ GeV/c. The nuclear modification factors are

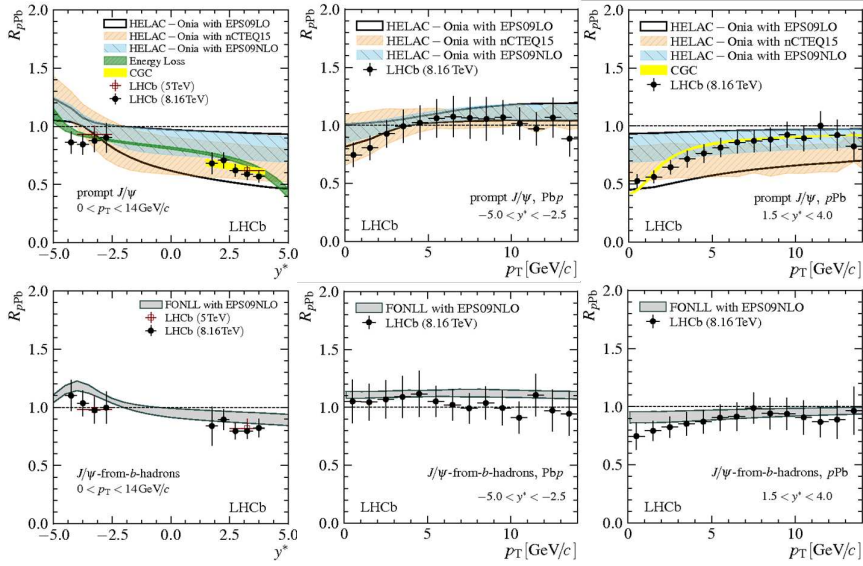


Figure 3. J/ψ nuclear modification factor, R_{pPb} : (left column) R_{pPb} integrated over p_T in the range $0 < p_T < 14$ GeV/c, as a function of y^* ; (middle and right columns) R_{pPb} integrated over y^* in the analysis range, as a function of p_T in PbP and pPb collisions, respectively. Top and bottom plots represent prompt and nonprompt J/ψ , respectively. The horizontal error bars indicate the bin widths and vertical ones the total uncertainties. The black circles are the values measured in this letter, the red squares the ones at $\sqrt{s_{NN}} = 5$ TeV from Ref. [1] and the coloured areas the theoretical computations from the models detailed in the text, with their uncertainties.

similar to those found at a collision energy of $\sqrt{s_{NN}} = 5$ TeV, but with increased precision. Although the presented measurements have improved precision, it is not possible to single out the main nuclear modification mechanism between different phenomenological models due to large uncertainties of nPDFs ones for charmonium production in proton-lead collisions at the TeV scale. This measurement of J/ψ production is the first step towards measurements of other charmonium states.

References

- [1] LHCb Collaboration, JHEP **02**, 072 (2014).
- [2] H.-Sh. Shao, Comp. Phys. Com. **184**, 2562 (2013); Comp. Phys. Com. **198**, 238 (2016).
- [3] B. Ducloue *et al.*, Phys. Rev. **D91**, 114005 (2015); Phys. Rev. **D94** 074031 (2016).
- [4] F. Arleo and S. Peigne, JHEP **03** 122 (2013).
- [5] LHCb Collaboration, Phys. Lett. B **774**, 159–178 (2017).
- [6] LHCb Collaboration, JINST **3**, S08005 (2008).
- [7] LHCb Collaboration, Int. J. Mod. Phys. **A 30**, 15300227 (2015).
- [8] T. Pierog *et al.*, Phys. Rev. **C92**, 034906 (2015); arXiv:1306.0121.
- [9] T. Sjostrand, S. Mrenna, P. Skands, Comp. Phys. Com. **178**, 852 (2008); arXiv:0710.3820.
- [10] ALICE and LHCb Collaborations, LHCb-CONF-2013-013; ALICE-PUBLIC-2013-002.
- [11] LHCb Collaboration, EPJ **C 71**, 1645 (2011); JHEP **06**, 064 (2013); JHEP **10**, 172 (2015).